Mean-field versus stochastic models for transcriptional regulation

R. Blossey and C. V. Giuraniuc
Biological Nanosystems, Interdisciplinary Research Institute, Lille University of Science and Technology, USR 3078 CNRS, Parc Scientifique de la Haute Borne, 50, Avenue Halley, F-59658 Villeneuve d'Ascq, France
(Received 2 April 2008; revised manuscript received 16 August 2008; published 10 September 2008)

We introduce a minimal model description for the dynamics of transcriptional regulatory networks. It is studied within a mean-field approximation, i.e., by deterministic ODE's representing the reaction kinetics, and by stochastic simulations employing the Gillespie algorithm. We elucidate the different results that both approaches can deliver, depending on the network under study, and in particular depending on the level of detail retained in the respective description. Two examples are addressed in detail: The repressilator, a transcriptional clock based on a three-gene network realized experimentally in *E. coli*, and a bistable two-gene circuit under external driving, a transcriptional network motif recently proposed to play a role in cellular development.

DOI: 10.1103/PhysRevE.78.031909 PACS number(s): 87.18.Cf, 87.10.Ed, 87.10.Mn

I. INTRODUCTION

Mathematical models for the dynamics of transcriptional regulation are traditionally formulated either in terms of ordinary differential equations [1,2], or by purely stochastic models, based on master equations [3] or by using the Gillespie algorithm [4]. Both the deterministic and stochastic descriptions average out spatial degrees of freedom and hence are more similar to each other than is often acknowledged. In recent years, a discussion has started on the effect of stochasticity on gene regulatory processes; exemplary studies are [5–9]. Indeed, already the fact that molecules involved in regulatory processes often exist only in small copy numbers can be significant for the dynamics of a given regulatory circuit, and stochastic effects like bursting may have an important role for cellular function [9].

Models of regulatory dynamics suffer also from another problem which is the lack of precise knowledge of reaction rates. Building dynamic models for a large number of network elements can induce further arbitrariness due to a lack of detailed knowledge of the interaction mechanisms involved. Approaches that aim to describe larger networks are often deliberately reductionist to become computationally tractable (see, e.g., [10], building on pioneering work by Glass, Kauffman, and Thomas [11,12]), and the result of such computations can then only be called "qualitative." The effect of these reduction schemes, which within a physics-based notion could also be subsumed under the notion of "coarse graining," therefore often lacks clarity as to what effect the approximations and/or simplifications have, since a general systematics is not available (an exemplary discussion of this issue can be found in [13]).

In this paper we address the question of what effect such a reduction scheme has on the dynamics of a given regulatory network in a systematic way. For this we start from a minimal model description for transcriptional regulatory networks which coarse grains as many regulatory layers as possible (although they could of course be added back in later). We note that this modeling philosophy is in contrast to the usual way models of transcriptional regulation are built in which first all available biochemical detail is considered and then reduced by way of approximation (as, e.g., in [14,15], and many other similar examples). We then formulate both a deterministic (mean-field) version and a stochastic version of the transcriptional dynamics. This approach allows us to study the dynamics of basically all fundamental classes of transcriptional networks relevant for prokaryotic organisms, although we only look at few-gene networks in detail here.

The outline of the paper is as follows. We first develop the kinetic reactions involved in transcriptional regulation. Subsequently, we formulate the corresponding deterministic and stochastic versions of the dynamics. A separate section of the paper is devoted to the application of both schemes to commonly encountered regulatory motifs [16]. Two examples are presented in more detail since they display richer structure: The repressilator, a three-gene network of inhibiting gates which acts as a genetic clock, previously realized experimentally in *E. coli* [17], and a regulatory motif with multiple inputs which was recently proposed to be relevant for regulatory processes in development [18]. For all of these systems, we compare the results of the deterministic calculations and their stochastic counterparts and evaluate the role different regulatory mechanisms play for the observed outcome.

II. GENE GATE MODEL

A. Transcriptional reactions

Our minimal model for transcriptional regulation consists in the definition of a computational element for each regulatory element (i.e., transcribing gene), which we call a gene gate. The basic possible types of gene gates are sketched in Fig. 1. Each gene gate is defined via its reaction kinetics. The "null gate" in part (1) of Fig. 1 is a gene in a state G which produces a protein output B at a rate ε, hence the kinetic reaction is written as

$$G \rightarrow_{\varepsilon} G + B. \tag{1}$$

The protein output can be degraded according to the reaction

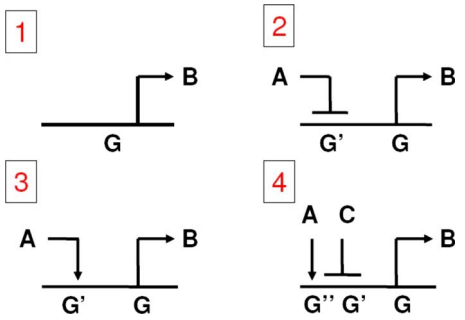

FIG. 1. (Color online) The four basic types of gene gates: (1) The null gate (a gate without control input); (2) the neg gate (repression of transcription); (3) the pos gate, activation of expression; (4) the posneg gate, a multi-input gate with one activating and one repressing input.

$$B \rightarrow_{\gamma} 0. \tag{2}$$

In an abbreviating notation we call this gate element null$(0;B)$ where inputs and outputs are separated by the semicolon.

In the next step we add a regulatory input to the null gate. Part (2) of Fig. 1 shows the resulting "neg gate" in which a transcription factor A inhibits the production of protein B upon binding. This is represented by the reaction

$$A + G \rightarrow_{r} G' + A. \tag{3}$$

This reaction corresponds to the formation of a transcription factor-DNA complex with zero lifetime; such an intermediate with a finite lifetime can of course be introduced as well but is not necessary for a minimal model of gene networks.

After this interaction, the gene in state G' is blocked in transcription and/or translation. In order to allow transcription again the gate must relax from its blocked state to its original transcribing state at a rate η,

$$G' \rightarrow_{\eta} G \tag{4}$$

to the state G in which transcription at a basal rate ε can occur. We call this gate the neg$(A;B)$ gate. The relaxation process from G' to G models the fact that a gene generally is not transcribed immediately after the break-up of a transcription factor-DNA complex; also note that within our minimal model of the gene gate, transcription and translation are lumped together.

Likewise we can model the activation of a gene upon binding of a transcription factor; part (3) of Fig. 1 shows the "pos gate." The binding reaction is identical, but the gene in state G' now behaves according to

$$G' \rightarrow_{\eta} G + B, \tag{5}$$

where the rate $\eta > \varepsilon$, i.e., the transcription and/or translation rate upon activation is larger than the basal rate. This is the pos$(A;B)$ gate.

Finally, part (4) of Fig. 1 shows a gate with multiple regulations which is in fact a commonly encountered situation, see, e.g., the *E. coli* network of transcriptional interactions reconstructed in [19]. For the posneg$(A,C;B)$ gate we must consider three gene states, G, G', and G'' with the reactions

$$C + G \rightarrow_{r_1} G' + C, \tag{6}$$

$$A + G \rightarrow_{r_2} G'' + A, \tag{7}$$

and the corresponding relaxation reactions

$$G' \rightarrow_{\eta_1} G, \tag{8}$$

$$G'' \rightarrow_{\eta_2} G + B. \tag{9}$$

It is clear from this scheme that for each additional regulatory function, a binding transcription factor and a corresponding gene state must be introduced.

Our minimal model obviously leaves out a number of regulatory levels such as

(i) complexation of transcription factors;

(ii) formation of the DNA-transcription factor complex;

(iii) DNA transcription and RNA translation are lumped together.

These regulatory mechanisms can, of course, be added to the list of reactions given above, and we will come back to this issue in the course of this paper.

B. Mean-field equations

Having listed the transcriptional reactions we now define a continuum description based on ordinary differential equations for the concentration of genes and proteins. We assume that the cell population can be considered as a "soup" containing the proteins as well as N copies of the gene G. We denote normalized concentrations by small letters $g \equiv [G]/N$, $b \equiv [B]/N$ with $[G] \equiv G/V$ (likewise for $[B]$) and keep the previous symbols for the kinetic constants (i.e., we include dependencies on cell volume V and gene copy number N where necessary; the difference to the kinetic reactions should be evident from the context). The two reactions of the null gate are then summarized by the ODE

$$\dot{b} = \varepsilon g - \gamma b. \tag{10}$$

For the regulated genes, an equation for g must be added. Since the N-gene gates present in our cell model must be either in state G or G', one has the conservation law $[G] + [G'] = N$. From the normalization we have $g + g' = 1$, and hence the neg gate is described by the two ODEs, Eq. (10) and

$$\dot{g} = \eta g' - rga = \eta[1 - (1 + \nu a)g], \tag{11}$$

where the conservation condition has been used, and $\nu \equiv r/\eta$.

The pos gate [part (3) of Fig. 1] is governed by the ODE's, Eq. (11), and

$$\dot{b} = \varepsilon g + \eta g' - \gamma b = \eta - (\eta - \varepsilon)g - \gamma b. \tag{12}$$

Finally, we consider the case of multiple regulations of a single gene, the simplest multi-input gate, the posneg-gate in part (4) of Fig. 1 with the three gene states, G, G', and G'', modifying the conservation condition to $g + g' + g'' = 1$. We can build up the gate reaction kinetics as before and obtain the system of ODE's

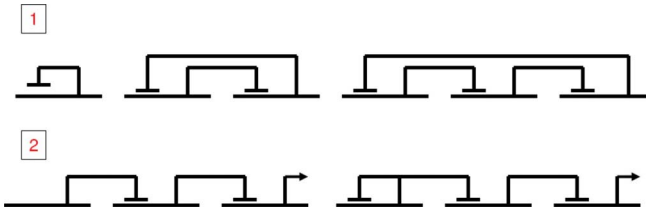

FIG. 2. (Color online) The two main classes of simple circuits: Circular (1) and linear (2). Shown are only the repressive circuits; activatory circuits and mixtures of both types can be built in a similar fashion. Circuits shown in (1): The autoinhibitive circuit, a bistable switch, the repressilator. Circuits shown in (2): A linear array and a linear array with a head feedback, hence a mixture of a circular and a linear circuit.

$$\dot{b} = \varepsilon b + \eta_2 g'' - \gamma b, \tag{13}$$

and

$$\dot{g}' = -\eta_1 g' + r_1 g c, \tag{14}$$

$$\dot{g}'' = -\eta_2 g'' + r_2 g a, \tag{15}$$

hence one has for g the equation $\dot{g} = -(\dot{g}' + \dot{g}'')$ which follows from the conservation of gene states.

At this point we stress that we have only considered the case of binding of a single protein A. In general, the binding of proteins is rather by multiprotein complexes (dimers or higher), which is one way to give rise to a Hill coefficient h when the complexation reaction is considered an equilibrium ("fast") reaction [20]. We could take this into account in our model by adding a corresponding complexation reaction in the reaction scheme. To be practical we here directly modify the ODE equation of the gene by replacing a by a^h with $h > 1$ to cover this more general case; in what follows, we consider h as a continuously variable parameter. It is well known that a Hill exponent >1 is essential for the dynamic behavior of simple gene circuits [21].

For the stochastic simulations we employ the Gillespie algorithm which is equivalent to the chemical master equation [4]. We combine the Gillespie method with the stochastic π-calculus, a process algebra originating in theoretical computer science [22–27]. For a brief introduction into the main ideas of the calculus, see the Appendix.

III. EXAMPLES

A. Basic circuits

We first discuss the elementary gene circuits that can be built from the above constructs. All simple transcriptional networks are either circular, linear or mixed circuits, see Fig. 2. The archetypal loops are the autoinhibitory and autoactivatory loops. The autoinhibitory loop $\mathrm{neg}(a;a)$ is shown in part (1) of Fig. 2. The ODE's governing its dynamics are

$$\dot{a} = \varepsilon g - \gamma a \tag{16}$$

and

$$\dot{g} = \eta g' - r g a = \eta[1 - (1 + \nu a^h) g]. \tag{17}$$

The natural first task is to look at nullclines and fixed points. The nullcline of g is determined by

$$g = \frac{1}{1 + \nu a^h}. \tag{18}$$

If we have $\dot{g}/\eta \approx 0$ and ν finite we can keep the circuit near the nullcline of g. Inserting the nullcline condition into the equation for a we find

$$\dot{a} = \frac{\varepsilon}{1 + \nu a^h} - \gamma a, \tag{19}$$

which is the common form of the Hill-type equation used in nonlinear dynamics descriptions of gene networks. This turns out to be a general feature of the gene gate approach: Near the nullclines of the gene gate states, $\dot{g} \approx \dot{g}' \approx \cdots \approx 0$, the circuit dynamics reduces to that of the standard Hill equations. This feature has an immediate consequence for the fixed points. The nuclline of a is given by

$$\frac{\varepsilon}{1 + \nu a^h} = \gamma a, \tag{20}$$

where the result for g has been used, and we thus find the standard fixed-point condition of the Hill equation for a. Since the left-hand side is a hyperbolic function in a, and the right-hand side is a linear function there is a unique fixed-point of the circuit.

The argument can be repeated for the autoactivatory loop $\mathrm{pos}(a;a)$ with the result

$$\dot{a} = \eta - \frac{\eta - \varepsilon}{1 + \nu a^h} - \gamma a = \frac{\varepsilon + r a^h}{1 + \nu a^h} - \gamma a, \tag{21}$$

which is the typical sigmoidal form of the activatory circuit. Therefore, we again find that the fixed points are given by a condition akin to the standard Hill-type equations, which for $h > 1$ gives rise to three fixed points.

The stability of the fixed points in the gene networks is not affected by the presence of the genes. We illustrate this for the bistable circuit composed of two neg gates, $\mathrm{neg}(a;b)|\mathrm{neg}(b;a)$, where the symbol "|" denotes the composition of two gates, see part (1) of Fig. 2. The equations of the circuit read as

$$\dot{a} = \varepsilon g_a - \gamma a \tag{22}$$

and

$$\dot{g}_a = \eta[1 - (1 + \nu b^h) g_a] \tag{23}$$

and likewise for $a \leftrightarrow b$. As is well known [21], the nonlinearity due to the Hill coefficient is needed for the system in order to display the fixed-point structure of the bistable switch; for a value of $h = 1$ as in our basic version of the gene gate model this is not the case. The stability of the fixed points follows from the eigenvalues of the matrix

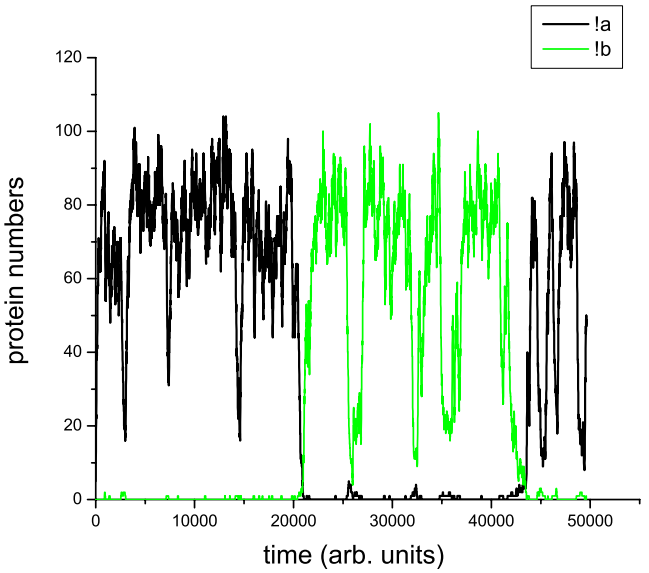

FIG. 3. (Color online) Switching in the stochastic bistable circuit without cooperativity. Simulation parameters are $r=1$, $\varepsilon=0.4$, $\eta=0.2$, $\gamma=5\times10^{-3}$. The inset indicates output on the π-calculus channels $!a$, $!b$, equivalent to protein numbers.

$$\Gamma_{fp}=\begin{pmatrix}-\gamma & \varepsilon & 0 & 0\\ 0 & -\chi & -\xi & 0\\ 0 & 0 & -\gamma & 0\\ -\xi & 0 & 0 & -\chi\end{pmatrix} \tag{24}$$

with

$$\chi\equiv\eta(1+\nu a_i^h),\quad \xi\equiv\frac{rha^{h-1}}{1+\nu a^h}. \tag{25}$$

Note that we are looking here at the stability of the symmetric fixed point for which $\chi_1=\chi_2$, $\xi_1=\xi_2$. For the bistable switch, this is the unstable fixed point intervening between the two stable fixed points, and its eigenvalues follow from the characteristic polynomial to Γ_{fp},

$$(\gamma+\lambda)^2(\lambda+\chi)^2=(\varepsilon\xi)^2. \tag{26}$$

Taking the root of this equation, one finds four real eigenvalues, two of which are negative, and two positive. The picture that emerges therefore is the usual instability in the space of protein concentrations a_1,a_2, while the genes do not contribute.

We close this section by commenting on results from the stochastic simulations. The basic loop and linear circuits (negative, positive) show fixed-point behavior similar to their deterministic counterparts [24]. For the bistable switch there is a notable difference: As was recently shown based on a master equation approach the stochastic dynamics of the bistable switch without cooperativity ($h=1$) displays both bistability and switching [28]. This behavior is easily reproduced with our Gillespie approach, see Fig. 3.

Before moving on to richer examples, we draw a brief intermediate conclusion for the gene gate model:

(i) If the deterministic gene circuit has a unique stable fixed point, the genes are "irrelevant" variables in the sense that they do not alter the location of the fixed point. They do, however, affect the transient dynamics (see below).

(ii) The deterministic dynamics requires Hill-type nonlinearity in order to show bistability and switching; for the stochastic dynamics, cooperativity is not needed.

B. Repressilator

Clearly, the dynamics of the genes does affect the systems transients, and as such the genes can indeed have a profound influence on the dynamics, as we now show. For this we look at a gene circuit whose stationary behavior is not governed by a simple fixed point, but by a limit cycle: The repressilator. The repressilator is the three-gene negative-feedback loop shown in part (1) of Fig. 2; this system has been realized experimentally as a synthetic gene circuit in *E. coli* [17], and it has recently been the topic of various modeling papers, employing both deterministic and stochastic approaches, e.g., [14,24,25,29].

The nonlinear dynamics of the repressilator in the nullcline space of the gates is described by the ODE

$$\dot{a}=\frac{\varepsilon}{1+\nu b^h}-\gamma a \tag{27}$$

with the equations for b and c to be obtained from the permutations $(a\to b,b\to c)$ and $(a\to c,b\to a)$. Since all parameters are assumed equal, the system has a symmetric fixed point, $a=b=c\equiv\bar{a}$. Testing the stability of this fixed point, the stability matrix reads as

$$\Gamma^{fp}=\begin{pmatrix}-\gamma & -\kappa & 0\\ 0 & -\gamma & -\kappa\\ -\kappa & 0 & -\gamma\end{pmatrix} \tag{28}$$

with $\kappa=\varepsilon h\nu\bar{a}^{h-1}/(1+\nu\bar{a}^h)^2$. The characteristic polynomial to this matrix is given by

$$(\gamma+\lambda)^3+\kappa^3=0, \tag{29}$$

so that the first eigenvalue is found to be

$$\lambda_1=-(\gamma+\kappa). \tag{30}$$

The two others are given by

$$\lambda_{2,3}=-\gamma+\frac{\kappa}{2}\pm i\frac{\kappa}{2}\sqrt{3}. \tag{31}$$

The condition for a Hopf bifurcation therefore is

$$\frac{\kappa}{2}=\gamma. \tag{32}$$

Making use of the fixed-point conditions one finds the relation

$$\bar{a}=\left(1-\frac{2}{h}\right)\frac{\varepsilon}{\gamma} \tag{33}$$

and hence the condition on the Hill exponent $h>2$ for the circuit in order to have a stable limit cycle.

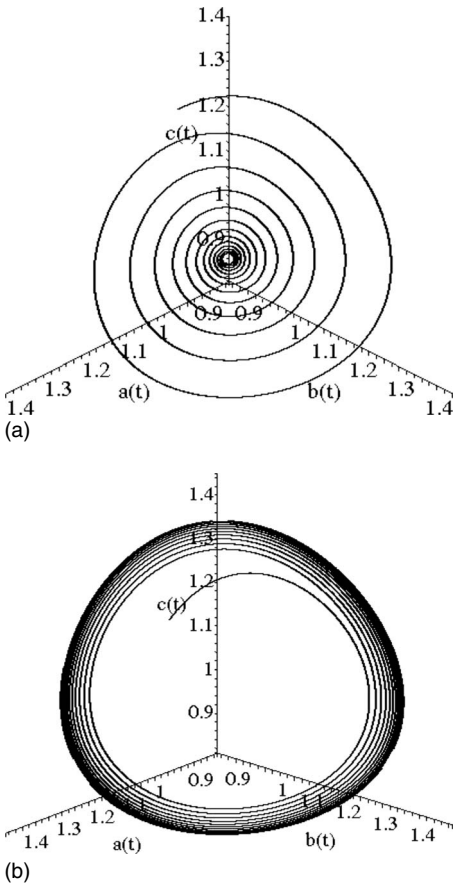

FIG. 4. Top: The repressilator dynamics without gene gates (fixed at the nullclines of the gates) for the parameters $r=1$, $\gamma=0.1$, $\varepsilon=0.3$, $\eta=0.9$, $h=3$. The limit cycle is absent, the fixed-point is stable. Bottom: Plot of the repressilator dynamics for the full system with identical parameters. The limit cycle persists in a wider range of parameters.

The stability analysis of this fixed point can be carried out analytically for the full gene gate circuit, i.e., keeping both the transcription factors and the three genes as dynamic variables. By symmetry, in fact, the calculation works for a circular circuit of n genes. The calculation amounts to generalize Eq. (26) so that

$$(\gamma+\lambda)^n(\lambda+\chi)^n+(-1)^{n-1}(\varepsilon\xi)^n=0 \tag{34}$$

with $n=3$ for the repressilator. This fixed-point condition is formally equivalent to that of the "leaky" repressilator discussed in [14], for which a condition $h>4/3$ was established. Within the full gene gate dynamics, the condition on h is thus weakened: The repressilator already oscillates for Hill exponent values less than 2. Even for the case $h=3$, e.g., when both the full and the restricted system show oscillatory behavior, the presence of the gene dynamics enlarges the oscillatory region in the space of protein concentrations (Fig. 4). The stability of the limit cycle in the space of parameters (ε,η) is summarized in Fig. 5.

By contrast, the stochastic repressilator without cooperativity displays a limit cycle behavior, as shown in Fig. 6 (top). The limit cycle appears as a symmetric triangle in the space

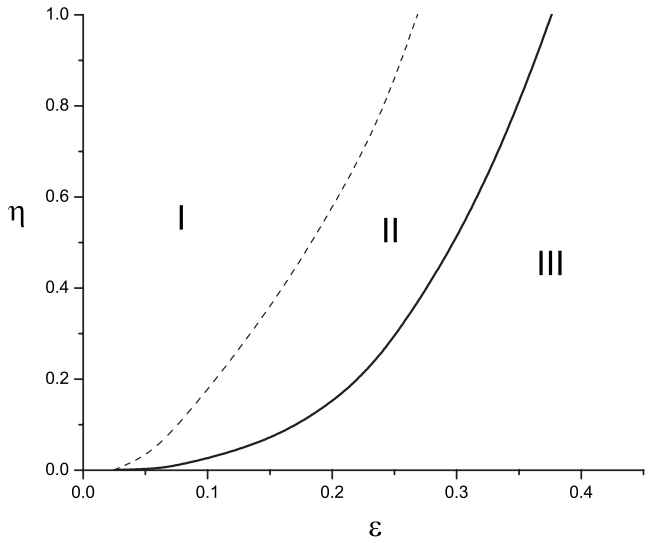

FIG. 5. Parameter regimes for the repressilator dynamics. I, stable fixed point; II, stable fixed point for the reduced system, limit cycle for the full system; III, limit cycle. Parameters are the same as in Fig. 4.

of transcription factor concentrations (a,b,c). The triangle is somewhat "fuzzy," reflecting the fluctuating nature of the concentrations. This fuzziness can be reduced by increasing the space of variables in the system. In a recent study, the effect of an inclusion of transcription factor cooperativity (dimerization and higher), or an inclusion of explicit RNA transcription and protein translation was studied. It was found that all of these mechanisms regularize the oscillatory behavior [25] and render the limit cycle less "fuzzy." Analogous findings for circadian clocks were reported earlier [30,31]. The corresponding limit cycle for the deterministic dynamics of the reduced system is shown in the bottom graph of Fig. 6. Here again a Hill coefficient $h=3$ has been assumed.

IV. MULTIINPUT GATES

A. Rewired repressilator

The stabilizing effect due to the presence of the gene gates persists in the presence of multiple inputs, in fact, it can even be reinforced. We observed this when considering a rewired repressilator shown in Fig. 7, in which an additional activatory loop has been added so that we have

$$\mathrm{neg}(c;b)|\mathrm{posneg}(c,b;a)|\mathrm{neg}(a;c). \tag{35}$$

In the case without genes, this means that one of the equations, say the one for a is replaced by

$$\dot{a}=\frac{\varepsilon+r_p c^h}{1+\nu b^h+\nu_p c^h}-\gamma a. \tag{36}$$

This "rewired" repressilator still has a unique fixed point (a,b,c), as follows from an analysis of the fixed-point conditions. The stability condition can be read off, as before, from the stability matrix which now reads as

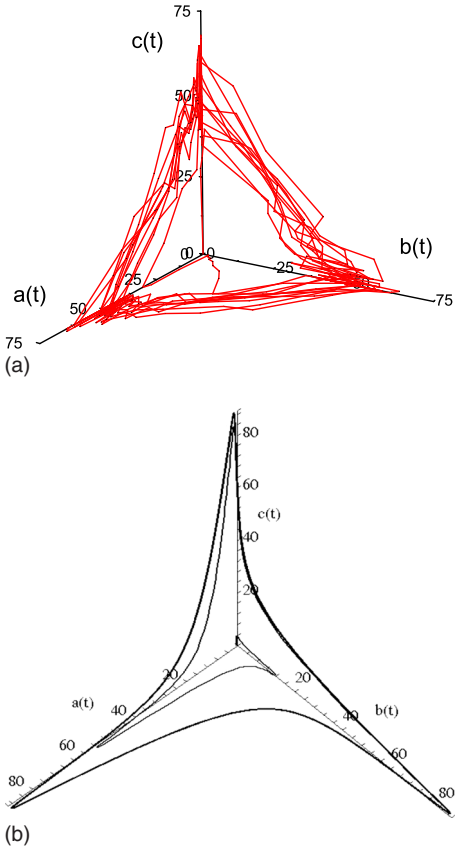

FIG. 6. (Color online) Top: The limit cycle of the stochastic repressilator. Simulation parameters are $r=r_p=1$, $\varepsilon=0.1$, $\eta=10^{-2}$, $\gamma=10^{-3}$. Bottom: The deterministic version for comparison (reduced system in region III of Fig. 5, parameters identical to the stochastic version, with $h=3$).

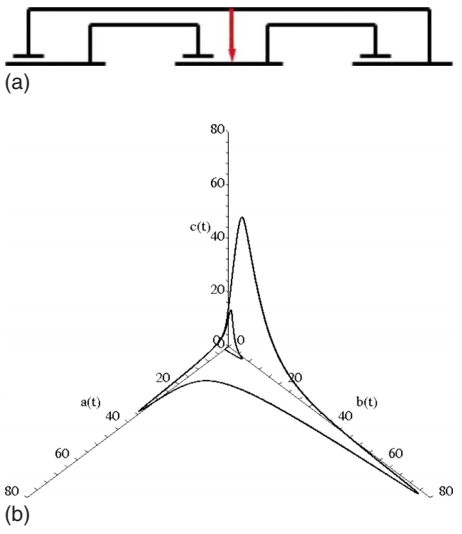

FIG. 7. (Color online) Top: The rewired repressilator, a positive loop is added (see arrow), so that one of the genes is doubly regulated. Bottom: The limit cycle of the (reduced) rewired repressilator circuit; the additional activation interaction breaks the symmetry, as discernable in the difference in maximal concentrations. Simulation parameters are $r=1$, $r_p=10^{-4}$, $\varepsilon=0.1$, $\eta_1=\eta_2=10^{-2}$, $\gamma=10^{-3}$, $h=3$.

$$\Gamma^{fp}=\begin{pmatrix}-\gamma & -\kappa_0 & \kappa_1\\ 0 & -\gamma & -\kappa_2\\ -\kappa_3 & 0 & -\gamma\end{pmatrix} \tag{37}$$

with

$$\kappa_0 \equiv \frac{\nu h b^{h-1}(\varepsilon + r_p c^h)}{(1+\nu b^h + \nu_p c^h)^2}, \tag{38}$$

$$\kappa_1 \equiv \frac{h c^{h-1}[r_p(1+\nu b^h) - \nu_p \varepsilon]}{(1+\nu b^h + \nu_p c^h)^2}, \tag{39}$$

$$\kappa_2 \equiv -\frac{\nu h c^{h-1}}{(1+\nu c^h)^2}, \tag{40}$$

$$\kappa_3 \equiv -\frac{\nu h b^{h-1}}{(1+\nu b^h)^2}. \tag{41}$$

Note that κ_1 can be both positive and negative. The characteristic polynomial reads as

$$(\gamma+\lambda)^3 + (\gamma+\lambda)\kappa_1\kappa_3 + \kappa_0\kappa_2\kappa_3 = 0 \tag{42}$$

which still has a pair of complex eigenvalues. The Hopf condition is given by

$$8\gamma^3 + 2\gamma\kappa_1\kappa_3 - \kappa_0\kappa_2\kappa_3 = 0. \tag{43}$$

The analysis of the full system, genes included, is clearly more involved than for the repressilator due to the increased number of variables. We have therefore studied the system only numerically and compared the reduced and the full version, as we did for the repressilator. Our calculations show that the reduced version (three ODE's for a,b,c) is less robust against rewiring than the gene gate version (seven ODE's): The stability limit of the limit cycle regime can differ by parameter values up to one order of magnitude. This finding is notable since in the presence of multiple regulations the number of gene states increases linearly with the number of inputs (neglecting still additional regulatory layers) and thus significantly enhances the complexity in modeling circuits with such elements. We close this section with Fig. 7 (bottom) which shows the limit cyle of the rewired repressilator for the reduced deterministic system ($h=3$). It illustrates that in general the presence of the additional positive loop breaks the $(a-b-c)$ symmetry between concentrations.

B. Multi-input circuit related to developmental regulation

In this final section we address a second example of a multi-input gate. It consists of a bistable switch built from two repressing gates which is placed under additional control by an activating input. Such motifs occur both in transcriptional regulation [19], but they have also been proposed recently to play a role in morphogen concentration-dependent cellular development [18]; our example is motivated by the latter case. The circuit dynamics is governed by the following ODE's (neglecting the gene gate dynamics since we are concerned with fixed-point dynamics only);

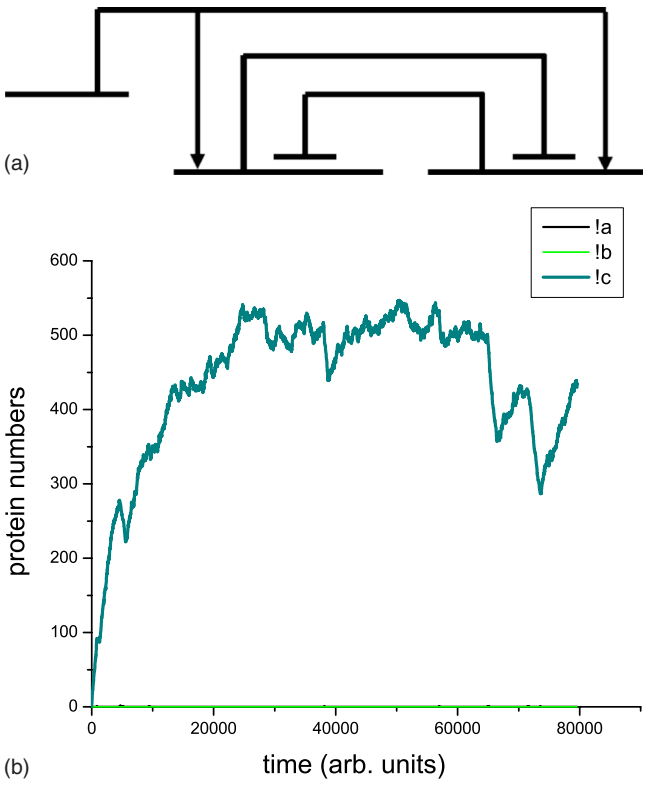

FIG. 8. (Color online) Top: The bistable switch under external control by a. Bottom: The system starts at zero concentrations of both proteins and enters the state with higher stability, as given by higher production rates. The signal c dominates widely over a,b which are indistinguishable from the baseline.

$$\dot{b} = \frac{\varepsilon_b + ra^n}{1 + \nu c^m + \nu_{ac} a^n} - \gamma b, \tag{44}$$

$$\dot{c} = \frac{\varepsilon_c + ra^n}{1 + \nu b^l + \nu_{ab} a^n} - \gamma c, \tag{45}$$

where m,n,l are the different Hill exponents. If the activating variable $a=0$, the system is the standard bistable switch, albeit asymmetric with respect to the parameters and nonlinearities, and it is this asymmetry which plays an important role—in Ref. [18], the supposed Hill coefficients have values of 3 and 6, respectively.

The effect of the variable a on the dynamics is easily understood. To simplify matters, we neglect a in the first equation and look at an asymmetric wiring. It actually does not matter whether we allow a to control one or both transcription factors b,c as long as a interacts with both in the same way and not via a different nonlinearity: The main symmetry-breaking effect is contained in the difference between the Hill coefficients controlling b and c.

Supposing further that we increase the concentration of a to levels where it dominates the concentration b so that we have for the fixed point in c,

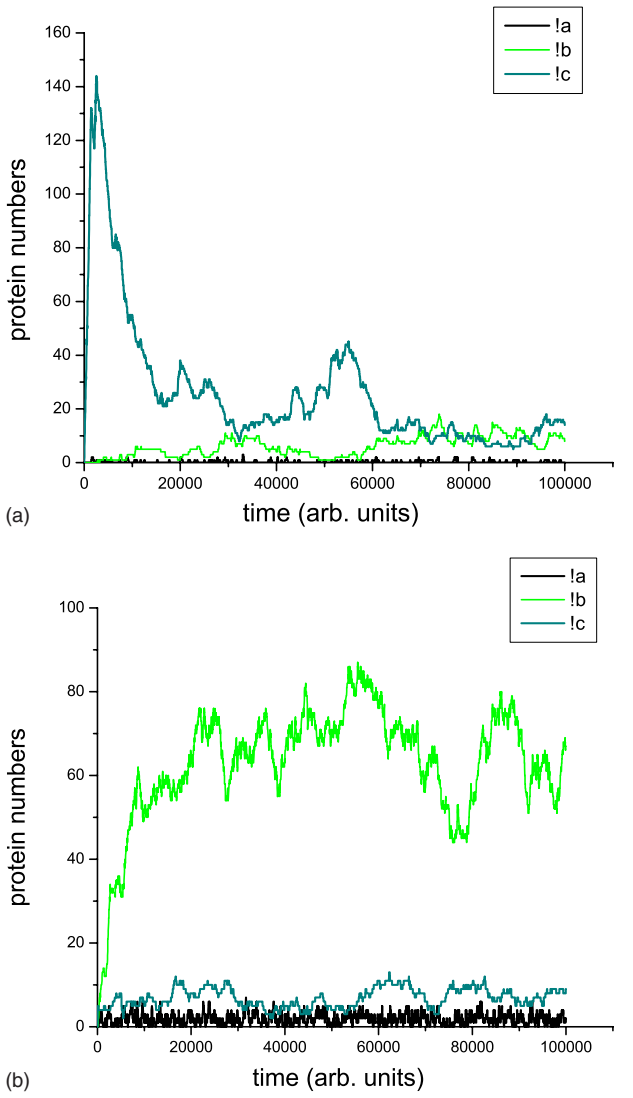

FIG. 9. (Color online) Top: A change of the activator transcription rate by one order of magnitude makes both proteins compete; note the concentration overshoots of the previously stable protein. Bottom: A further increase of the activator transcription rate makes the system switch between the two states. Simulation parameters are (bottom): $r=1$, $\varepsilon_a=10^{-3}$, $\varepsilon_b=0.1$, $\varepsilon_c=10^{-3}$, $\eta_{ab}=2\times10^{-3}$, $\eta_{ac}=2\times10^{-2}$, $\eta=2\times10^{-1}$, $\gamma_a=5\times10^{-3}$, $\gamma=2\times10^{-4}$.

$$c_0 = \frac{1}{\gamma}\frac{\varepsilon_c + ra^n}{1 + \nu_{ab} a^n} \underset{a\gg1}{\rightarrow} \frac{\eta_{ab}}{\gamma}. \tag{46}$$

Thus, the fixed-point concentration of the repressing variable c_0 is locked to that of a and approaches an asymptotically constant value. Correspondingly, this brings the fixed-point level of b down and under firm control of a: The system ceases to be bistable, and locks into a stable state under control of a. The possible relevance of this mechanism for a transcriptional circuit in development is evident: Increasing a can force the system to switch in a concentration dependent way.

In the nonlinear dynamics case, this switch is therefore brought about by the vanishing of a fixed point; again, this

situation is different in the stochastic setting. For comparison, Figs. 8 and 9 show our results of the stochastic simulations for the circuit

$$\text{null}(a)|\text{posneg}(a,b;c)|\text{posneg}(a,c;b) \tag{47}$$

without any cooperative nonlinearity, as for the repressilator. The progression of dynamic behaviors in Fig. 8 (bottom) to Fig. 9 (top and bottom) is controlled by the average concentration level of a, which increases from one figure to the next by one order of magnitude since the transcription rate is increased by this factor. In Fig. 8 (bottom) the switch enters the more stable of the two states; in Fig. 9 (top) the additional input a makes the concentration levels b and c compete with each other. This behavior is observed within a large parameter range, in which bursts in concentration c can occur at random times within a wide time interval (see the concentration peak at around 55.000 a.u.), and are finally controlled by a. In Fig. 9 (bottom) the system has switched to a dominant concentration of b and the concentration of the previously dominant transcription factor c is now fully controlled by a. Note the difference in concentration levels of all proteins in the figures.

V. DISCUSSION AND OUTLOOK

In conclusion we have proposed a minimal model description for gene regulatory networks based on the notion of the gene gate, first proposed in Ref. [24]. We studied the dynamics of simple gene networks in both a mean-field and a stochastic version, with characteristically different results.

(i) If the system dynamics is stable fixed point only, a reduced deterministic description ignoring the degree of freedom of the gates is sufficient in the sense that the fixed point is not altered by the presence of the genes. But if this is the case, the latter are indeed "irrelevant." In order to represent faithfully the fixed-point structure of the network, a Hill-type nonlinearity may be needed (like for the bistable switch circuit). However, within a stochastic description fluctuation effects induced by the genes (promoters) might affect fixed-point locations [32], or the stability of bistable switches [33–36].

(ii) If the system displays a limit cyle, the gene gates are relevant, as is any other additional regulatory layer to determine the parameter range of oscillations. In general the limit cycle regimes depends on the whole set of parameter values, Hill coefficient included. In particular this means that in multi-input regulations in which additional gene states must be accounted for, the parameter space can extend significantly.

(iii) If the system dynamics is fixed point, the stochastic version obeys this without any need for cooperative effects. The same holds true for limit cyle behavior. Additional regulatory layers also enlarge the phase space but in a trivial way. By contrast, they affect oscillatory behavior by regularizing the oscillations.

In our view these results have interesting consequences on the philosophy of modeling gene regulatory networks in suggesting a different coarse approach. Computational models of large networks can be built by abstracting away all regulatory layers to a level where the remaining network can still faithfully represent the system characteristics. Network motifs that have a more sensitive dynamic behavior—like limit cycles, as shown here—are more sensitive to modeling assumptions. Finally, we remark that in view of our results, modeling attempts combining deterministic and stochastic aspects should be considered with care [37].

ACKNOWLEDGMENTS

We thank Luca Cardelli, Andrew Phillips, and Yasushi Saka for discussions.

APPENDIX: SIMULATIONS IN STOCHASTIC π-CALCULUS

The Gillespie algorithm can, of course, be implemented in various different programming languages. What then are the main ideas and advantages of the π-calculus?

The π-calculus is a formal system in which each computation is represented by a communication over input and output channels. The communicating objects are called "processes." Computation by communication within π-calculus can be understood as an alternative to, e.g., functional computation as realized in the λ-calculus. The π-calculus is Turing complete: It can therefore realize any possible computation [22].

For our application, the calculus allows us to represent each gene gate by a computational process

$$\text{gate}(x;y) \tag{A1}$$

with its corresponding input(s) x and output(s) y; e.g., the repressing gate in part (2) of Fig. 1 is written as $\text{neg}(a;b)$ where the input channel a represents the repression of transcription by transcription factor a, and b is the corresponding output. All other reactions, e.g., the degradation process of b, are bound to this process and contained in its definition.

The scheduling of inputs and outputs on a gate are calculated in the usual fashion by the standard Gillespie algorithm, as adapted to the π-calculus [24–26].

One main technical advantage of the calculus is, in fact, that its syntax and semantics are perfectly adapted to a "compositional" build-up of the transcriptional networks. In our context this permits us to express (and compute) a composed circuit, such as the repressilator, by a parallel process

$$\text{neg}(c;b)|\text{neg}(b;a)|\text{neg}(a;c). \tag{A2}$$

The second main advantage (although not exploited for the small systems studied here) is that it can reduce the computational complexity of a system of n kinetic reactions, which is of order n^2, to linear order. The interested reader is referred to Refs. [24,25] for more details, written in a way accessible to a physics-trained audience. The simulation results presented here were obtained with the public domain software SPIM, downloadable with documentation and examples [27]. The details of the implementation of the Gillespie algorithm in the dedicated software SPIM are discussed in the supplementary materials of [24,25].

[1] A. Goldbeter, *Biochemical Oscillations and Cellular Rhythms* (Cambridge University Press, Cambridge, United Kingdom, 1996).
[2] *Computational Cell Biology*, edited by C. P. Fall, E. S. Marland, J. M. Wagner, and J. J. Tyson (Springer, Heidelberg, Germany, 2002).
[3] N. van Kampen, *Stochastic Processes in Physics and Chemistry* (North-Holland, Amsterdam, 2007).
[4] D. T. Gillespie, J. Phys. Chem. **81**, 2340 (1977).
[5] J. M. G. Vilar, H. Y. Kueh, N. Baarkai, and S. Leibler, Proc. Natl. Acad. Sci. U.S.A. **99**, 5988 (2002).
[6] P. S. Swain, M. B. Elowitz, and E. D. Siggia, Proc. Natl. Acad. Sci. U.S.A. **99**, 12795 (2002).
[7] M. B. Elowitz, A. J. Levine, E. D. Siggia, and P. S. Swain, Science **297**, 1183 (2002).
[8] J. Paulsson, Nature (London) **427**, 415 (2004).
[9] J. Paulsson, Phys. Life. Rev. **2**, 157 (2005).
[10] H. de Jong, J. Geiselmann, C. Hernandez, and M. Page, Bioinformatics **19**, 336 (2003).
[11] L. Glass and S. A. Kauffman, J. Theor. Biol. **39**, 103 (1973).
[12] R. Thomas, J. Theor. Biol. **42**, 565 (1973).
[13] R. Bundschuh, F. Hayot, and C. Jayaprakash, Biophys. J. **84**, 1606 (2003).
[14] S. Müller, J. Hofbauer, L. Endler, C. Flamm, S. Widder, and P. Schuster, J. Math. Biol. **53**, 905 (2006).
[15] S. Widder, J. Schicho, and P. Schuster, J. Theor. Biol. **246**, 395 (2007).
[16] U. Alon, *An Introduction to Systems Biology* (CRC Chapman and Hall, London, United Kingdom, 2006).
[17] M. B. Elowitz and S. Leibler, Nature (London) **403**, 335 (2000).
[18] Y. Saka and J. C. Smith, BMC Evol. Biol. **7**, 47 (2007).
[19] M. Madan Babu and S. A. Teichmann, Nucleic Acids Res. **31**, 1234 (2003).
[20] J. N. Weiss, FASEB J. **11**, 835 (1997).
[21] J. L. Cherry and F. R. Adler, J. Theor. Biol. **203**, 117 (2000).
[22] R. Milner, *Communicating and Mobile Systems: The π-Calculus* (Cambridge University Press, Cambridge, 1999).
[23] C. Priami, A. Regev, W. Silverman, and E. Shapiro, Inf. Process. Lett. **80**, 25 (2001).
[24] R. Blossey, L. Cardelli, and A. Phillips, T. Comp. Sys. Bio. **IV**, 99 (2006).
[25] R. Blossey, L. Cardelli, and A. Phillips, HFSP J. **2**, 17 (2008).
[26] A. Phillips and L. Cardelli, *Computational Methods in Systems Biology*, Lect. Notes Comput. Sci. Vol. 4695 (Springer, New York, 2007), p. 184.
[27] http://research.microsoft.com/~aphillip/
[28] A. Lipshtat, A. Loinger, N. Q. Balaban, and O. Biham, Phys. Rev. Lett. **96**, 188101 (2006).
[29] A. Loinger and O. Biham, Phys. Rev. E **76**, 051917 (2007).
[30] D. Gonze, J. Halloy, and A. Goldbeter, Proc. Natl. Acad. Sci. U.S.A. **99**, 673 (2002).
[31] D. Gonze, J. Halloy, and P. Gaspard, J. Chem. Phys. **116**, 10997 (2002).
[32] J. Paulsson, O. G. Berg, and M. Ehrenberg, Proc. Natl. Acad. Sci. U.S.A. **97**, 7148 (2004).
[33] P. B. Warren and P. R. ten Wolde, Phys. Rev. Lett. **92**, 128101 (2004).
[34] R. J. Allen, P. B. Warren, and P. R. ten Wolde, Phys. Rev. Lett. **94**, 018104 (2005).
[35] A. M. Walczak, J. Onuchic, and P. G. Wolynes, Proc. Natl. Acad. Sci. U.S.A. **102**, 18926 (2005).
[36] M. J. Morelli, S. Tanase-Nicola, R. J. Allen, and P. R. ten Wolde, Biophys. J. **94**, 3413 (2008).
[37] M. Scott, T. Hwa, and B. Ingalls, Proc. Natl. Acad. Sci. U.S.A. **104**, 7402 (2007).